Oceanologia 63 (2021) 531—544

Available online at www.sciencedirect.com

ScienceDirect

journal homepage: www.journals.elsevier.com/oceanologia

ORIGINAL RESEARCH ARTICLE

Machine learning methods applied to sea level predictions in the upper part of a tidal estuary

Nicolas Guillou*, **Georges Chapalain**

Laboratoire de Génie Côtier et Environnement (LGCE), Cerema, Plouzané, France

Received 16 March 2021; accepted 8 July 2021
Available online 21 July 2021

KEYWORDS
Multiple regression methods;
Artificial neural network;
Multilayer perceptron;
Elorn;
Landerneau;
Western Brittany

Abstract Sea levels variations in the upper part of estuary are traditionally approached by relying on refined numerical simulations with high computational cost. As an alternative efficient and rapid solution, we assessed here the performances of two types of machine learning algorithms: (i) multiple regression methods based on linear and polynomial regression functions, and (ii) an artificial neural network, the multilayer perceptron. These algorithms were applied to three-year observations of sea levels maxima during high tides in the city of Landerneau, in the upper part of the Elorn estuary (western Brittany, France). Four input variables were considered in relation to tidal and coastal surge effects on sea level: the French tidal coefficient, the atmospheric pressure, the wind velocity and the river discharge. Whereas a part of these input variables derived from large-scale models with coarse spatial resolutions, the different algorithms showed good performances in this local environment, thus being able to capture sea level temporal variations at semi-diurnal and spring-neap time scales. Predictions improved furthermore the assessment of inundation events based so far on the exploitation of observations or numerical simulations in the downstream part of the estuary. Results obtained exhibited finally the weak influences of wind and river discharges on inundation events.

* Corresponding author at: Cerema, Direction Risques, Eau et Mer, HA, Laboratoire de Génie Côtier et Environnement (LGCE), 155 rue Pierre Bouguer, Technopôle Brest-Iroise, BP 5, 29280, Plouzané, France.
E-mail address: nicolas.guillou@cerema.fr (N. Guillou).
Peer review under the responsibility of the Institute of Oceanology of the Polish Academy of Sciences.

Production and hosting by Elsevier

https://doi.org/10.1016/j.oceano.2021.07.003

1. Introduction

Artificial Intelligence analysis techniques and methods are commonly exploited in a wide range of applications including navigation safety, agriculture optimisation, design of mechanical structures, etc. Characterised by remarkable learning ability, noise tolerance and generalisability, these advanced approaches offer new horizons compared to traditional engineering methods, and are therefore recognised as one of the pillars of future economic and industrial developments. Thus, these powerful methods are also playing an increasing role in the study of coastal processes, and their importance is reinforced by a growing number of observational available datasets (Beuzen and Splinter, 2020). Among the different applications in marine systems, particular attention was dedicated to the prediction of flood and streamflow in watersheds, thus exploiting the potential of machine learning algorithms to mimic the highly non-linear complex hydrodynamic and hydrological processes (Humphrey et al., 2016; Noori and Kalin, 2016; Rezaeianzadeh et al., 2013; Tsakiri et al., 2018). In marine and estuarine environments, these advanced approaches were primary applied to the prediction of coastal storm surge (Chao et al., 2020; Hashemi et al., 2016; Sahoo and Bhaskaran, 2019) and a series of environmental parameters and variables including, among others, the significant wave height (Asma et al., 2012; Deo et al., 2001), the sea surface temperature (Wolff et al., 2020) or the water turbidity (Renosh et al., 2017; Wang et al., 2021b). In relation to its highly-predictable characteristics, particular attention was also dedicated to tide forecasting with applications in harbours disseminated along the coastline by comparing traditional harmonic analysis techniques with machine learning methods (French et al., 2017; Lee and Jeng, 2002; Liu et al., 2019).

However, few investigations based on machine learning were applied to sea level forecasting in the upper part of estuaries where the conjunction and interaction between spring tide, storm surge and river discharge may induce inundation of surrounding urbanised areas. Indeed, these aspects are traditionally considered by relying on high-resolution numerical simulations with complex interactions between (i) tide-induced hydrodynamics and storm surge, (ii) bathymetry, wetting-drying areas and seabed roughness, and (iii) meteorological forcings (including surface wind and atmospheric pressure) (Peng et al., 2004; Pinheiro et al., 2020; Shih et al., 2019). In spite of the advanced knowledge reached about the physics of estuarine inundations, this type of simulation requires important computational resources with numerous treatments applied to input and output data, and complex model calibrations. It relies furthermore on an extensive amount of input data including especially a refined spatial distribution of the water depths along the main estuarine channel as well as in bordering wetting-drying areas, and this involves extensive measurement campaigns. For these reasons, such advanced simulations are not available in all areas, especially in small estuaries characterised by a lower population density, and therefore reduced financial support for the development of such numerical tools. Thus, the preliminary estimation of inundation events in the upper part of the estuary derived, most of the time, from the predictions of peak water levels downstream, based on (i) tidal harmonic recomposition (which may involve a large amount of observed data) or (ii) predictions from a large-scale model (which may also require high computational efforts) (French et al., 2017). These rough evaluations ignore furthermore the amplification and deformation of the tidal wave in the upper estuary, thus resulting in an approximation of inundation events upstream (Wang et al., 2019).

The present investigation complements these different applications by assessing the suitability and capability of machine learning algorithms to predict the evolution of water depth and river overflows in the upper part of a small estuary located in western Brittany (France, Figure 1). As an explanatory investigation to the implementation of advanced machine learning approaches, the attention was dedicated to simple methods including multiple regression approaches and basic neural networks. The site of application is the city of Landerneau, upstream the Elorn estuary which discharges in the macro-tidal environment of the bay of Brest (Beudin et al., 2014). With a watershed surface of 260 km^2 and an annual mean water discharge of 6 $m^3\ s^{-1}$, this estuary accounts for around 20% of total river fresh waters inputs to the bay of Brest (Beudin et al., 2014; Tréguer et al., 2014). The river extends over a total length of 56 km, but it is characterised by a weir 14 km away upstream of its mouth, at the "Pont de Rohan" in the city of Landerneau. Thus, upstream of this location, the influence of the tide appears only for high tides. Furthermore, numerous maritime developments, initially conducted to support the ancient harbour activity of the city, have led to the constriction of estuary natural width from 1.8 km at its mouth in the bay of Brest to less than 40 m in the city Landerneau. The estuary shows also large wetting-drying areas revealed at low tide in its downstream part. These result in significant deformation and amplification of the tide and coastal surge along the Elorn estuary as exhibited by the comparison between observed surface elevations in the harbour of Brest and in the city of Landerneau, downstream the "Pont de Rohan" (Figure 2). Thus, the city is regularly subjected to inundation events that impact the safety of inhabitants, the economic activity, urban transport, and surrounding goods and materials. There is therefore a need for the improved efficient forecast of peak water levels in the upstream part of the Elorn estuary to help services and operators of the city in mitigating the effects of inundation events.

Following these objectives, we considered two types of machine learning algorithms applied to the predictions of water depth elevation in the city of Landerneau: (i) multiple regression methods based on linear and polynomial regression functions, and (ii) an Artificial Neural Network (ANN), the MultiLayer Perceptron (MLP). Multiple regression methods are traditionally considered to investigate the functional relationships among variables whereas ANN is a biologically inspired computational model dedicated to processing connections between a series of neurons (in hidden layers) and to approaching complex highly non-linear problems. This investigation relied on three-year observations of water depth elevation in the city of Landerneau. Without a refined hydrodynamic numerical simulation of the estuary, city services have so far exploited predictions from a large-scale tidal model to encompass the evolution of the

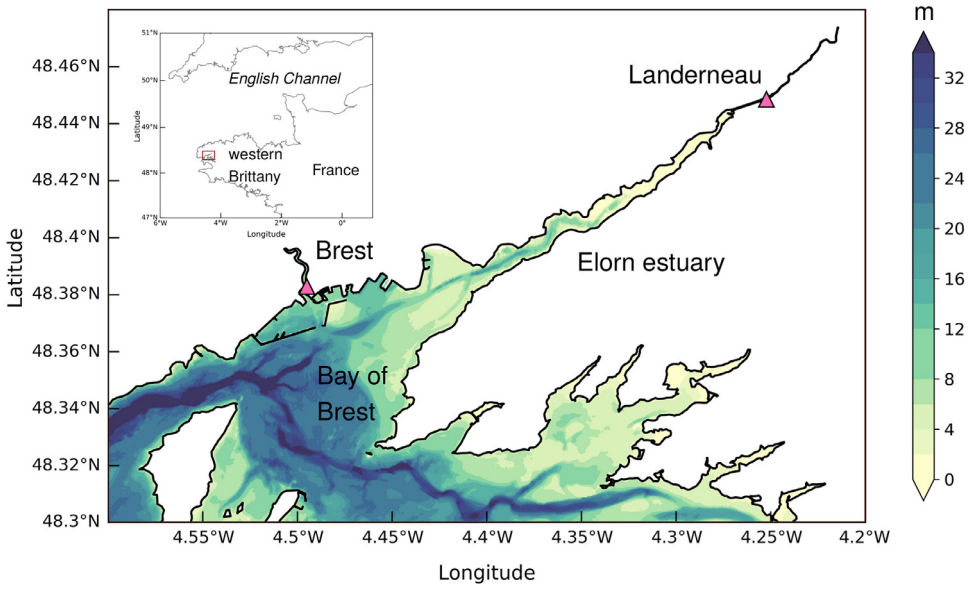

Figure 1 Area of interest with locations of tidal gauges in the harbour of Brest and the city of Landerneau (shown with triangles).

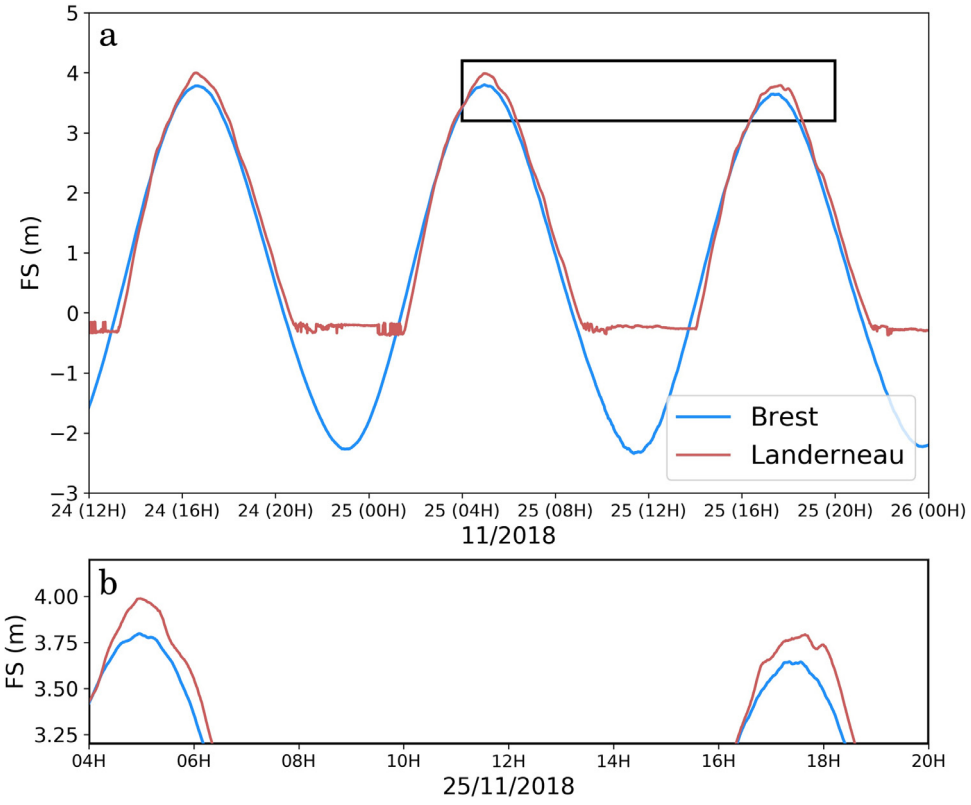

Figure 2 Time series of free-surface elevation observed during spring conditions in Brest and in Landerneau. These evolutions are shown with respect to the french IGN reference ("Institut Géographique National"). In Landerneau, observations at low tide show the seabed elevation.

water level in the upper part of the estuary. These large-scale predictions were assessed with respect to tidal-gauge observations in the harbour of Brest downstream the Elorn estuary. Thus, results here obtained with machine-learning algorithms were compared to these downstream observations, taken as reference values for approaching the water level in the city of Landerneau without refined numerical hydrodynamic simulations of the Elorn estuary.

In a view of approaching river overflow and inundation events in Landerneau, the attention was dedicated to pre-

dictions of peak water depths reached during high tides. We considered four input variables for these advanced algorithms in relation to tidal and coastal surge effects on sea level in the estuary: (i) the French tidal coefficient as an indicator of tidal range, (ii) the atmospheric pressure at mean sea level, (iii) the wind velocity near the sea surface and (iv) the river discharge. Particular attention was furthermore dedicated to the sensitivity of predictions to these input parameters. Whereas such investigation was specific to the Elorn estuary, it provided further insights about the potential of machine learning as an efficient and rapid alternative to complex high-resolution numerical simulations with high-computational efforts for the predictions of water depth in the upper part of estuaries. Thus, these methods may be exploited in broader locations to give information to urban planners, administrators and policy makers for mitigating inundation risks in urbanised areas upstream estuaries while optimizing the design of infrastructures and supporting the development of an alert system.

The paper is organised as follows. Section 2 successively describes the available observations of sea surface elevation here exploited (Section 2.1), the machine learning algorithms considered (Section 2.2) and the associated dataset and input variables (Section 2.3.2). Section 3 presents and discusses results obtained by focusing on the training, validation and testing of algorithms. Thus, section 3.1 describes the selection of (i) multiple regression methods with particular attention on polynomial functions and (ii) MLP for different numbers of hidden layers and neurons per layer. Section 3.2 discusses the final testing of models selected with respect to observations in the city of Landerneau. Particular attention was dedicated to the approach of inundation events characterised by the highest sea levels. Section 3.3 finally investigates the sensitivity of these machine learning algorithms to input parameters.

2. Material and methods

2.1. Tidal gauge observations

The investigation relied on observations of free-surface elevation at two locations: (i) off the Elorn estuary in Brest harbour and (ii) in the upper part of the estuary in Landerneau (Figure 1). The first station implemented along the quayside of Brest harbour accounts for nearly 300 years of observations, thus representing one of the longest observed time series of tidal free-surface elevation in the world (Wöppelmann et al., 2008). These measurements are conducted within a well attached to the quayside which filters the effects of local waves and wind on the evolution of the sea surface. Recorded data are therefore considered to result from the only contribution of tide and storm surge. Data exploited here were provided, at a time interval of one minute, by the French navy SHOM ("Service Hydrographique et Océanographique de la Marine") (SHOM, 2021). The second station was implemented by the Cerema ("Centre d'études et d'expertise sur les risques, l'environnement, la mobilité et l'aménagement") and its Laboratory of Coastal Engineering and Environment (Cerema-LGCE, 2021) as part of a global monitoring system of environmental parameters in the bay of Brest and the Elorn estuary. The instrumentation system consists of a Vega radar level sensor (Vegaplus WL 61) implemented in the city of Landerneau along the quayside downstream the "Pont de Rohan". Data were acquired since 02 March 2017 with a time step varying between 30 seconds and 1 minute. The period of observations here exploited covers more than three years, thus extending until 25 June 2020. Due to maintenance operations and system malfunction during its development, different periods were missing from observations (Figure 3). However, these three-years measurements (between 2017 and 2020) integrate different inundation events in Landerneau, thus representing a valuable source of information to investigate risks of river overflow and associated extreme water levels.

As exhibited before, observations in Brest harbour filter the contribution of local wave agitation and surface wind, which results in relative uncertainties in the approach of the total water depth. However, these measurements are traditionally exploited for the setup and validation of tidal harmonic algorithms and database, as well as large-scale tide-surge models in western Brittany. Thus, these data may be considered as representative of the best potential predictions of sea level variations in the downstream part of the Elorn estuary. Without refined numerical hydrodynamic simulations within the estuary, these observations were therefore taken as reference values liable to be exploited in preliminary studies of river overflow assessment in the city of Landerneau.

2.2. Machine learning algorithms

With the objective of assessing the potential of machine learning approaches for predicting the sea level in the upper part of the Elorn estuary, we considered and compared three algorithms: two multiple regression methods, (i) the Multiple Linear Regression (MLR) and (ii) the Multiple Polynomial Regression (MPR), and an Artificial Neural Network, (iii) the MultiLayer Perceptron (MLP). More advanced ANN are also proposed in the literature, such as Recurrent Neural Networks with the capability to be trained using back-propagation through time. However, in spite of numerous advantages to approach highly non-linear problems, these algorithms show an important degree of complexity in comparison with regression methods and MLP which makes it difficult to conduct a relevant assessment between these different approaches. These advanced methods are furthermore primary adapted to forecasting of time-series variables with historical dependency (Fan et al., 2020; Wang et al., 2021a; Wolff et al., 2020). Thus, further differences exist in the input features between (i) these advanced ANN and (ii) the basic regression methods and MLP. In the objective of considering similar input parameters for the different algorithms, advanced ANN were therefore ignored from the present investigation. Machine learning approaches here considered were finally implemented by relying on the Deep Learning Python libraries Scikit-learn and Keras (Keras, 2021).

2.2.1. Multiple regression methods

Machine learning algorithms relied on a supervised training dedicated to learning relationships between input data and an output targeted variable. Thus, MLR is one of the

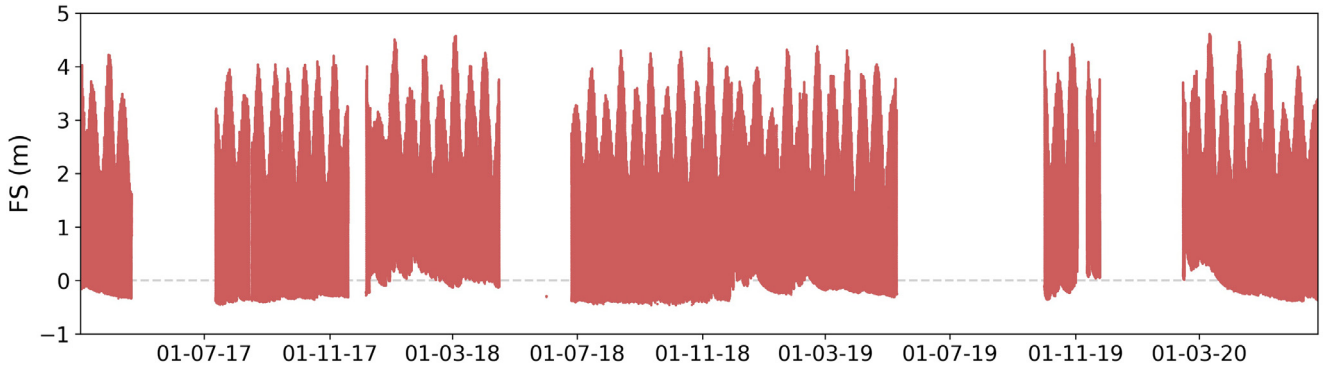

Figure 3 Time series of free-surface elevation observed between 2017 and 2020 in Landerneau. These evolutions are shown with respect to the french IGN reference ("Institut Géographique National").

simplest supervised learning technique applied to determine the best linear trend lines between a series of input parameters and an output variable. For a series of n observations, input variables may be noted as $(x_{1,j}, \ldots x_{p,j})$ with p the number of input parameters and $j \in [1, n]$ the observation considered. y_j is the targeted variable for this observation. With these notations, the estimated linear regression function takes the form $f(x_{1,j}, \ldots, x_{p,j}) = \alpha_0 + \sum_{i=1}^{i=p} \alpha_i x_{i,j}$, and the multiple regression method determines the different values α_i, with $i \in [0, p]$, which minimize the sum of squared residuals between this function and the targeted variable for all observations. In comparison with MLR, MPR relies on a polynomial regression function. Thus, in addition to linear terms like $\alpha_i x_{i,j}$, with $[i, j] \in [1, p] \times [1, n]$, the regression function may include non-linear terms such as $\beta_{i,2} x_{i,j}^2$ or $\beta_{i,3} x_{i,j}^3$ for polynomial functions of degrees 2 or 3. This type of regression function makes it easier to adjust the targeted observations. However, methods adopted in MLR and MPR appear very similar if terms such as $x_{i,j}^2$ or $x_{i,j}^3$ are considered as input variables. Indeed, by doing so, the polynomial regression problem is solved as a linear problem.

Beyond forecasting, multiple regression methods may also be exploited to characterise the importance of input parameters on the output variable, thus providing further insights about the physical mechanisms and processes governing the evolution of the targeted parameter. Nevertheless, such application requires the exploitation of independent inputs so that an input variable may be modified without impacting the other variables (Azencott, 2019). Multiple regression methods were applied in a series of applications in the coastal and marine environments. Asma et al. (2012) relied on multiple linear regression methods to characterise the significant wave height on the west coast of India by exploiting a series of meteorological parameters including the wind speed and gust, and the atmospheric pressure. Beyond providing accurate predictions with error rate below 0.1, MLR approached the performances of artificial neural network models. More recently, Ali et al. (2020) applied MLR to predict significant wave height off the coast of Australia. Optimized by covariance-weighted least squares estimation algorithm, the model was able to provide reliable forecast at one lag of 30-min scale with Root-Mean Squared Error below 0.10 m. In the present investigation, we considered MLR and MPR with polynomial regression function of degrees 2 and 3 (Table 1).

Table 1 Description of machine learning models considered.

Model	Parameters and hyperparameters
MLR	
MPR	deg=2
	deg=3
MLP	1 hidden layer with 3, 4, 5 and 10 neurons
	2 hidden layers with 3, 4, 5 and 10 neurons
	3 hidden layers with 3, 4, 5 and 10 neurons

2.2.2. Multilayer perceptron

However, in spite of the physical interpretation reached, simplified regression models may have limitations to resolve real-world applications characterised by (i) highly nonlinear relationships between the input features and the outcome, and (ii) further interactions between these input features. Thus, more advanced ANN methods are considered in relation to its adaptability to complex multivariate nonlinear problems. MLP refers to one of the simplest class of ANN and consists basically of three types of layers of nodes including (i) the input layer with the series of input features, (ii) the hidden layers with neurons (also called perceptrons) receiving the input values with a weight and transferring the output to the next layer via a non-linear activation function and (iii) the output layer with the targeted variable (Figure 4). Thus, MLP results from a complex combination of non-linear activation functions of weighted inputs, and such a parametric model provides a highly non-linear approximation of the final estimate. The activation function considered between hidden layers for this application was the Rectified Linear unit (ReLu) particularly suited for addressing the vanishing and exploding gradient problems (Nair and Hinton, 2010). A linear function was also considered for the output layer. The training process consists of two phases. The first phase is the feed-forward stage during which the information is conveyed from the input to the output layers and modified with the weighted and activation operations of the hidden layers. The second reverse phase consists in

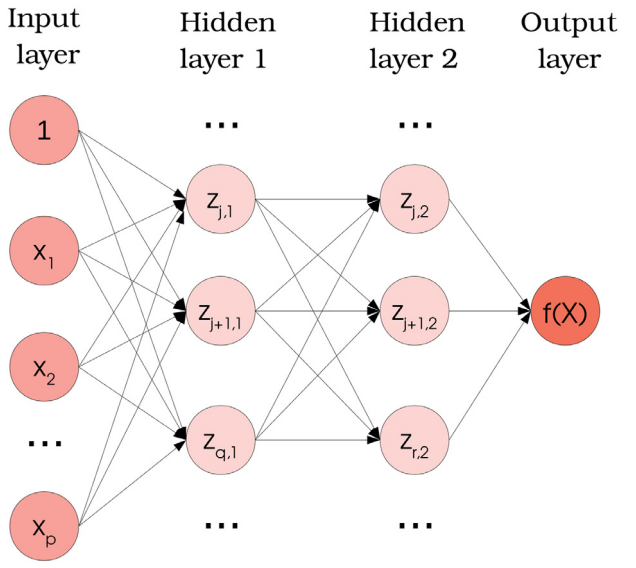

Figure 4 Architecture of a MultiLayer Perceptron (MLP) with two hidden layers. p refers to the number of input variables. q and r refer to the numbers of perceptrons in the first and second hidden layers, respectively.

back-propagating the error to the hidden and input layers, thus updating the weights of connection between neurons. In the present investigation, this stage relies on the efficient Adaptive moment estimation (Adam) version of stochastic gradients descent which optimizes the mean squared error loss function (Kingma and Ba, 2015). Thus, MLP is considered as a feed-forward ANN with a back-propagation learning algorithm. Further details about MLP are available, among others, in Azencott (2019) and Kumar Paramasivan (2019). MLP was used by Manero et al. (2019) to forecast the spatio-temporal distribution of the wind and associated energy in a series of locations disseminated over the United States of America (USA). They obtained a good approach of the wind velocity magnitude for a time horizon of less than 3 hours with median values of the coefficient of determination over 0.7. More recently, Wolff et al. (2020) relied on MLP to predict the short and long-term evolutions of the sea surface temperature with hindcast input and atmospheric data. This investigation revealed comparable performances between MLP and state-of-the-art physics-based model simulations from the European Centre for Medium Weather Forecasting, thus capturing seasonal patterns and approaching short-term variations associated with atmospheric forcing. MLP was also exploited by Feng et al. (2020) to wave forecasting in Lake Michigan (USA). The algorithm was able to predict wave conditions (significant wave height and peak period) with results comparable to a third-generation spectral wave model implemented in this lacustrine environment.

Neural networks such as MLP are more complex models than MLR or MPR, and are thus very difficult to optimize. However, we conducted a preliminary assessment of the performance of MLP with respect to the number of hidden layers and neurons per layer. Whereas increasing the depth of the network may improve the performance on the training data, it may also increase the risk of over-fitting, therefore reducing the generalisation potential of the trained algorithm. Thus, we considered different configurations by varying the number of hidden layers in the range [1,2,3] and the number of perceptrons per layer in the range [3,4,5,10] while setting aside regularisation considered in over-fitting configuration (Table 1). This results in a series of twelve MLP to be trained and compared. Given the important range values of input variables (Section 2.3.2), these features were standardised by removing the mean and scaling to unit variance. The learning algorithm worked finally 100 times (number of epochs, cycles of learning when the network weights are updated, estimated from preliminary investigations of the loss function) over the entire trained dataset (batch size set to one) to reach an accurate estimate of the gradients, and the random seed number was fixed to guarantee the reproductibility of results obtained.

2.3. Output and input data

2.3.1. Output data

The present investigation aims at characterising the inundation events in the city of Landerneau by relying on machine learning techniques. Thus, instead of focusing on the complete time series of sea level variation in the upper part of the Elorn estuary (which will require the treatment of a huge amount of data), the attention was dedicated to the maximum sea level reached during the successive high tides, and the approach of these maxima with a series of explanatory variables. Time series of observations were therefore treated to extract the maximum levels reached during high tides in Landerneau and Brest. This results in a time series of n=1536 targeted variables y_j (with $j \in [1, n]$) for maximum levels in the city of Landerneau and this corresponds nearly to 800 days of continuous observations during the three years considered (between 02 March 2017 and 25 June 2020).

2.3.2. Input data

As consistency during the analysis is of utmost importance to conduct a reliable comparison between the different approaches, we relied on the same input data for machine learning algorithms. Input data were selected in relation to the potential influence on the evolution of sea level in the upper part of the estuary. Thus, in order to characterise the influence of tidal amplitude, we selected the French tidal coefficient C_{tide} as the first input parameter. This parameter, which varies between 20 and 120, is a global indicator of semi-diurnal tidal range variations along the coast of France with the principal objective to inform the population about tidal magnitude. Its value is calculated by the French navy SHOM from the ratio between (i) the semi-diurnal tidal range of the harmonic formula and (ii) the average tidal range value for equinoxic spring tides, being equal to 6.1 m in Brest harbour where this coefficient is computed (Simon, 2007). This tidal coefficient is therefore representative of tidal range variations in the area of interest. Nevertheless, highest sea levels result also from the influence of meteorological conditions which impact coastal surge (which adds to tide-induced sea levels). For this reason, we also included the atmospheric pressure P_{atmos} and the wind speed. Data were extracted from the operational analysis time series of the Climate Forecast System (CFSv2, National Oceanic and Atmospheric Administra-

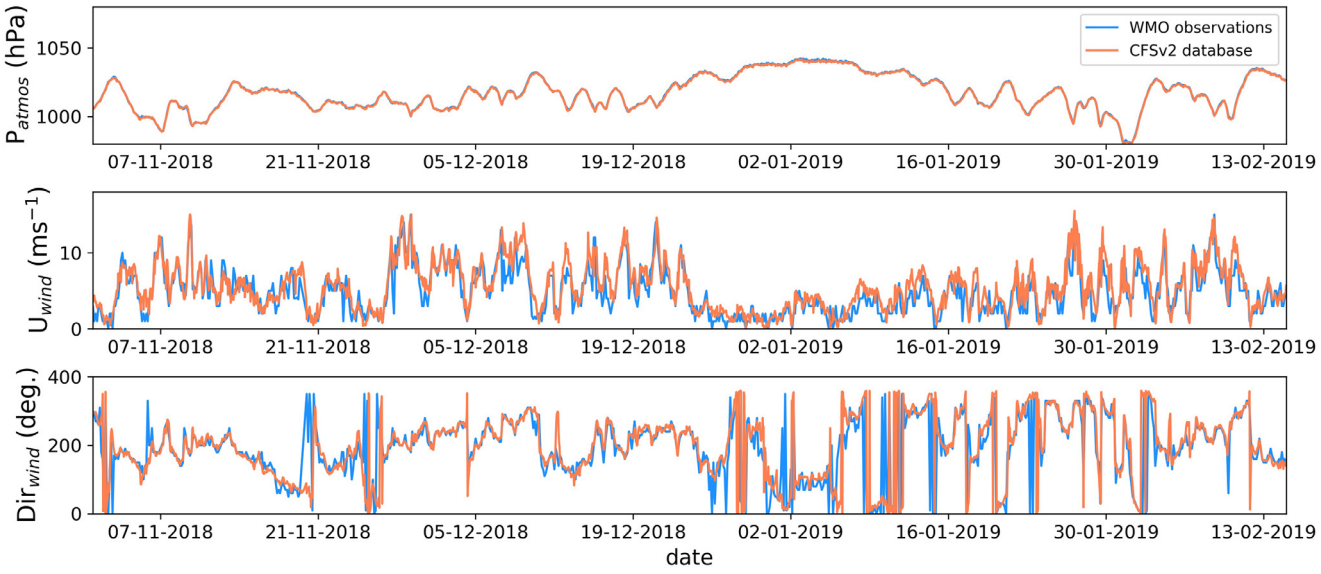

Figure 5 Time series of atmospheric pressure, wind magnitude and direction (nautical convention) from CFSv2 database and WMO observations. Dates indicated correspond to midnight.

Table 2 Description of input variables considered in machine learning algorithms.

Input variables	Description	Source
C_{tide}	French tidal coefficient	SHOM (2021)
P_{atmos}	Atmospheric pressure at mean sea level	NOAA (2021)
$Wind_{proj}$	Wind velocity projection along the orientation of the Elorn estuary	NOAA (2021)
$River_{flow}$	River flow	Banque Hydro (2021)

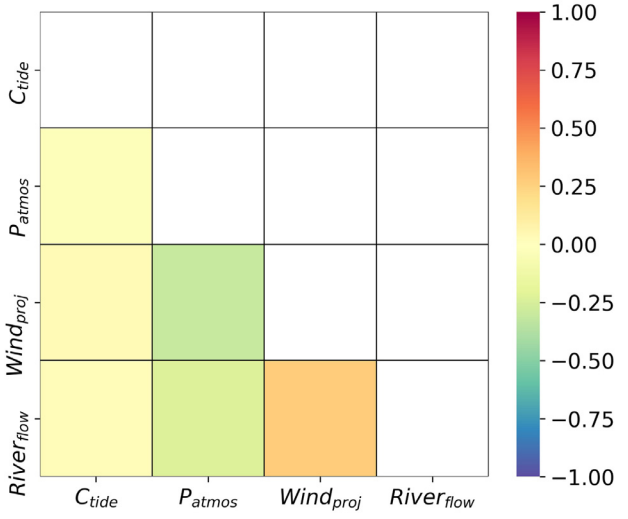

Figure 6 Matrix of Spearmann correlation coefficients between input features of machine learning algorithms. Results are naturally shown for the lower part of this symmetrical matrix.

tion) (NOAA, 2021; Saha et al., 2014). In spite of a rough spatial resolution of 0.5°, a relative good agreement was found between these data and data from international surface observations messages of the World Meteorological Organization for the city of Brest (WMO, 2021) (Figure 5). However, the wind direction is a particular parameter whose evolution can not be characterised like its magnitude. Thus, the value of 0 is similar to the value of 2π. For this reason, the input parameter selected was the projection of the wind velocity along the orientation of the Elorn estuary $Wind_{proj}$. The upstream river flow $River_{flow}$ was finally considered by relying on hourly observations, at the upstream station of "Pont-ar-Bled", gathered in the database of Banque Hydro (2021). These different input variables are listed in Table 2.

2.3.3. Data pre-processing and partitioning

The potential correlations between the four input variables were investigated by relying on the Spearman coefficient (Figure 6). As noticed by Asma et al. (2012), the effects of meteorological factors such as sea level atmospheric pressure may appear in the wind speed. However, results obtained confirmed that input variables are weakly correlated with each other with correlation coefficients being restricted below 0.30. Thus, these variables were exploited as input for the multiple regression methods and MLP (Section 2.2). Input variables were interpolated at times of observed maximum sea levels y_j (with $\boldsymbol{j} \in [1, \boldsymbol{n}]$ and n=1536) in the city of Landerneau. The application of machine learning algorithms requires furthermore to divide the input dataset into three parts: (i) training for the supervised learning of methods considered, (ii) validation for the selection of the different models obtained, and (iii) testing for

Table 3 Scoring for the evaluation of peak sea levels during high tides in the city of Landerneau for the validation dataset based on the exploitation of observations in Brest and multiple regression methods. The multiple regression methods which provided the best predictions over the validation dataset are exhibited in bold.

Model/method	MAE	RMSE	R^2
Brest observations	0.200 m	0.213 m	0.900
MLR	**0.099 m**	**0.126 m**	**0.965**
MPR (deg=2)	**0.098 m**	**0.125 m**	**0.965**
MPR (deg=3)	0.105 m	0.134 m	0.960

the final evaluation of the model selected. To meet these requirements, input datasets were first divided into training and validation in the ratio 40:30%, thus setting aside the final 30% of dataset. After the training of the 15 models considered (Table 1), the validation dataset was exploited to select the best algorithms in multiple regression methods and MLP. The selected models were then re-trained and tested in the ratio 70:30% of the total dataset and finally evaluated with respect to inundation forecasting in the city of Landerneau. Such a data partitioning guarantees an evaluation of the prediction capabilities of machine learning algorithms on a new dataset (the final 30% not initially exploited) independent of training data. Performances of the different algorithms were finally evaluated with a series of statistical and scoring metrics including the Mean Absolute Error (MAE), the Root-Mean Squared Error (RMSE) and the coefficient of determination R^2 between observations and predictions.

3. Results and discussion

3.1. Model validation and selection

3.1.1. MLR and MPR

The three multiple regression methods were first trained and validated in the ratio 40:30% of the total dataset, thus setting aside the final 30% of available data between 02 March 2017 and 25 June 2020 (which were exploited for the final testing of models selected in Section 3.2). Over this initial validation dataset, these three algorithms improved the predictions of peak water levels reached during high tides in Landerneau in comparison to the exploitation of downstream observations in Brest (Table 3). Thus, MAE and RMSE from multiple regression methods were nearly halved compared to scoring from Brest observations. The associated coefficient of determination R^2 reached values over 0.96 for MLR and MPR whereas it was restricted to 0.90 for Brest observations. Indeed, in spite of a high correlation with the evolution of the tide in Landerneau, downstream observations did not include the deformation and amplification of the tide and coastal surge along the Elorn estuary. As exhibited by Wang et al., 2019, these downstream observations were found to underestimate peak sea levels upstream (Figures 7 and 8).

Table 4 Scoring for the evaluation of peak sea levels during high tides in the city of Landerneau for the validation dataset based on MLP. The MLP which provided the best predictions over the validation dataset are exhibited in bold.

# of hidden layers	# of neurons/ layer	MAE	RMSE	R^2
1	3	0.101 m	0.130 m	0.962
1	4	0.103 m	0.132 m	0.961
1	5	0.103 m	0.130 m	0.963
1	10	0.104 m	0.133 m	0.961
2	**3**	**0.099 m**	**0.128 m**	**0.963**
2	4	0.101 m	0.130 m	0.963
2	5	0.102 m	0.129 m	0.963
2	10	0.107 m	0.135 m	0.959
3	3	0.100 m	0.129 m	0.963
3	4	0.101 m	0.129 m	0.963
3	**5**	**0.100 m**	**0.127 m**	**0.964**
3	10	0.105 m	0.135 m	0.960

As Brest observations were considered for the setup and validation of tidal harmonic database and large-scale tide-surge models, we may expect increased differences by relying on these benchmarch predictions for the approach of peak sea levels in Landerneau. Multiple regression methods represent therefore an interesting alternative to the exploitation of these downstream predictions. Weak differences were furthermore obtained between the three multiple regression algorithms. Increasing the degree of the polynomial regression function was found to reduce the quality of predictions, and nearly similar results were obtained between the MLR and MPR (with a degree of 2 for the polynomial regression function).

3.1.2. MLP

Results from MLP considered appeared in fairly good agreement with the validation dataset, thus confirming the performance of ANN for such multi-variable application (Table 4). MLP scoring was comparable to values obtained from multiple regression methods and provided also improved estimations of peak sea levels in the upstream Elorn estuary in comparison with the exploitation of Brest observations, downstream. Whereas very weak differences were obtained between the twelve MLP tested, slightly better performances were identified for the two configurations of (i) two hidden layers and three neurons/layer and (ii) three hidden layers and five neurons/layer. This confirmed that MLP may also provide good estimates with a limited number of hidden layers and inter-connections between perceptrons (Messikh et al., 2017). Indeed, as exhibited by Lee and Jeng (2002) for the predictions of tidal sea level around Taiwan, more hidden layers increase the complexity of neural networks and may result in substantial errors and uncertainties in predictions of tidal sea level.

3.1.3. Final selection

However, as trained multiple regression methods and MLP provided similar results, it was very difficult to refine the selection. For this reason, we retained the regression meth-

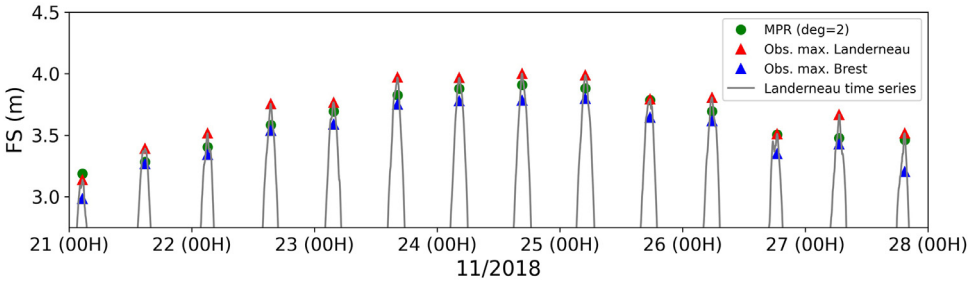

Figure 7 Time series of free-surface elevation observed in Landerneau with observations in Brest and predictions in Landerneau (from MPR with deg=2) of maxima reached during high tides during spring tidal conditions. These comparisons were shown over the initial validation dataset.

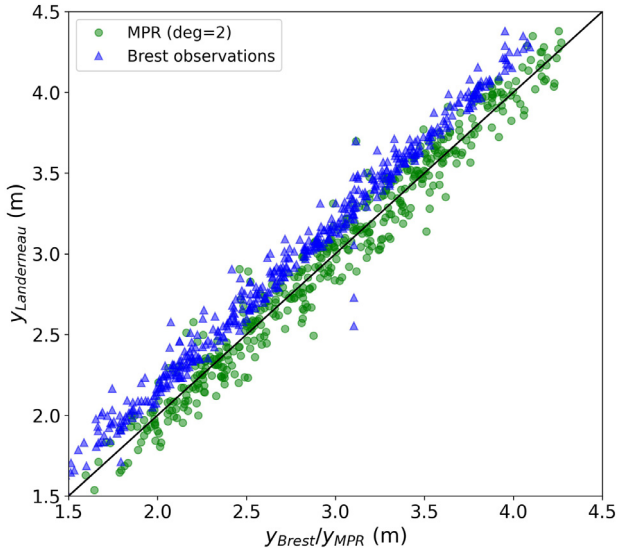

Figure 8 Correlation, over the initial validation dataset, between maxima observed and predicted (from MPR with deg=2) during high tides in the city of Landerneau (green circles). Correlation between maxima observed in the city of Landerneau and observed in Brest harbour (blue triangles).

ods and the MLP that resulted in the best scoring: (i) the MPR with a polynomial regression function of degree two and (ii) the MLP with three hidden layers and five perceptrons/layer. These two machine learning algorithms were therefore considered for the model testing and the approach of inundation events in the city of Landerneau.

3.2. Model testing

As described in Section 2.3.3, the two models selected were re-trained and tested in the ratio 70:30% of the total dataset. Thus, the tested dataset (30% of the total dataset) was considered for the first time for the evaluation of selected machine learning algorithms. Confirming previous estimations (Section 3.1), weak differences were obtained between the MPR and MLP models retained (Table 5). These weak differences were consistent with results obtained by Asma et al. (2012) for the predictions of the significant wave height with MLR and MLP. Slightly better estimations were however obtained in relation to an increased number of input variables for the training of the two algorithms (70% of the total dataset here against 40% for the initial models selection). Thus, both algorithms reproduced the temporal variations of sea levels maxima during high tides at both semi-diurnal and spring-neap time scales (Figure 9).

The capability of both models to approach inundation events in the city of Landerneau was investigated by setting up a threshold value for river overflow. This value was determined by relying on observations of dock elevations on both sides of the Elorn river both upstream and downstream the “Pont de Rohan” and the threshold of 4.08 m was retained (Figure 10). This corresponds to the dock elevations downstream the “Pont de Rohan”. This value may seem a bit weak in comparison with the value of 4.35 m retained by city services, thus resulting in an overestimation of impacting inundation events. Indeed, a sea level close to this critical value will have reduced effects whereas a sea level greatly exceeding this value will result in important inundation events. However, retaining such a weak value makes it easier to characterise highest sea levels as inundation events. Thus, by adopting the limit of 4.08 m, both models were able to identify sea level observations exceeding 4.35 m as inundation events, mainly as differences between predictions and observations remained below 0.11 m (Figure 11). Increased differences were, however, obtained for sea levels over 4.08 m. Thus, both machine learning algorithms were found to underestimate the sea levels reached during these events which resulted in a characterisation of around 72% of observed inundations (over a total of 32 events that exceeded the value 4.08 m for the tested dataset). These percentages decreased to 69.7% by including cases where machine learning models predicted values over 4.08 m whereas observed values remained below this limit (Table 5). Such tendency to under-predict at the upper end of sea level was also obtained by French et al. (2017) for the estimation of coastal surge inundation at estuarine harbours in the United-Kingdom. Thus, differences obtained here for the total water depth may be explained by an tendency to under-predict highest storm surges in the upper part of the Elorn estuary. Nevertheless, in spite of these differences, these machine learning models allowed a big step towards the approach of inundation events in the city of Landerneau, especially if compared with the exploitation of downstream observations which resulted in a characterisation of only 37.5% of these events (Table 5).

Table 5 Scoring for the evaluation of peak sea levels during high tides in the city of Landerneau for the tested dataset obtained from training and testing in the ratio 70:30% of the total dataset.

Model/method	MAE	RMSE	R^2	# of inundation events captured
Brest observations	0.208 m	0.221 m	0.903	37.5%
MPR (deg=2)	0.094 m	0.118 m	0.972	69.7%
MLP (3 hidden layers and 5 neurons/layer)	0.095 m	0.123 m	0.970	69.7%

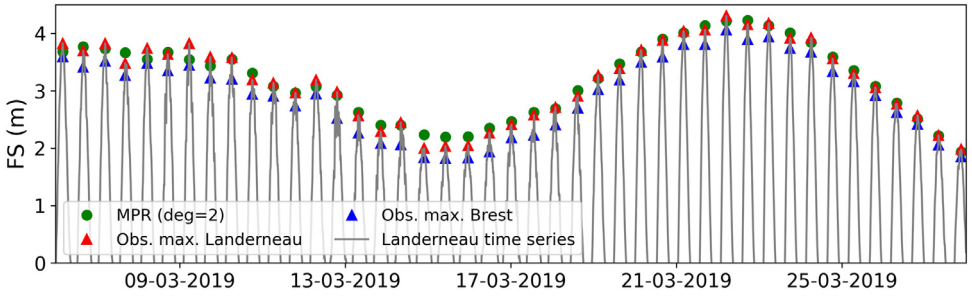

Figure 9 Time series of free-surface elevation observed in Landerneau with observations in Brest and predictions in Landerneau (from MPR with deg=2) of maxima reached during high tides during a spring-neap tidal cycle. Predictions from MPR result from the new partition of trained and tested dataset in the ratio 70:30% and are shown for tested dataset only.

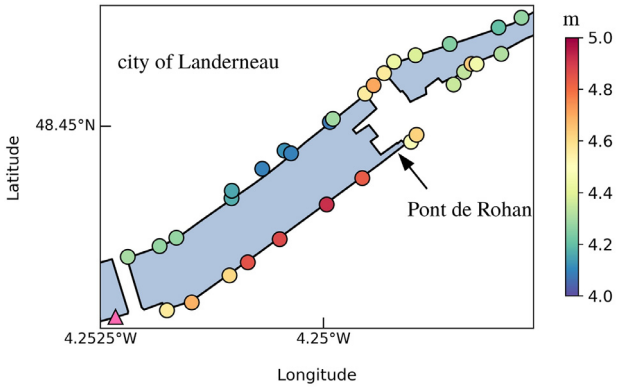

Figure 10 Dock elevations (shown with respect to the french IGN reference) on both sides of the Elorn estuary both upstream and downstream the "Pont de Rohan" in the city of Landerneau. The location of the instrumentation system is shown with a triangle.

3.3. Sensitivity analysis

In a view of exploiting these advanced machine learning algorithms, further insights were provided about the sensitivity of predictions to input variables. Our analysis relied on the MPR with a polynomial regression function of degree two over the re-trained and tested ratios 70:30% of the total dataset. The resulting models showed naturally different evaluations of sea levels maxima in the city of Landerneau (Table 6). The inclusions of upstream river discharges and wind were found to have weak effects on predictions. However, increased differences were obtained by including the atmospheric pressure. Indeed, the tidal coefficient was the input variable with the strongest correlation with sea level variations in Landerneau, thus modulating maxima sea levels with respect to tidal range. Nevertheless, its solely inclusion was found to increase the trend of predictions to overestimate observations, thus reducing the performance of this model for the approach of inundation events as exhibited by associated scoring (Table 6 and Figure 12). The inclusion of both tidal coefficients and atmospheric pressure restricted this tendency resulting in nearly similar scoring for MAE, RMSE and R^2 as those obtained for the complete inclusion of the four input variables. It led furthermore to a better approach of inundation events. Such improved predictions may be explained by the importance of atmospheric pressure on coastal surge which added to the tidal level. Thus, with the inclusion of these two variables, different peak elevations may be reached for the same tidal coefficient. These results exhibited furthermore the reduced effects of wind and upstream river flow on sea levels variations at the measurement location considered in the city of Landerneau. Inundation events appeared therefore as a result of marine submersion rather than the combination of marine submersion and river flood.

This sensitivity study exhibited also the practicality of these machine learning algorithms liable to provide a refined estimation of inundation events in an upstream tidal estuary with a limited number of input variables. Thus, unlike numerical physical models, the bathymetry was not required to approach maximum water levels in the upper part of the Elorn estuary. Furthermore, with an exception for upstream river discharges that derived from observations, all other input variables were extracted from database repository derived from large-scale meteorological models. It is therefore possible to approach inundation events in this local environment by relying on input data at coarse spatial resolutions, and this may be applied to forecast applications based on large-scale climate database. Thus, this method may be considered in broader locations to approach future inundation events by exploiting climate forecast and tidal-range predictions. However, as exhibited before, water levels in the upper part of the estuary is influenced by a se-

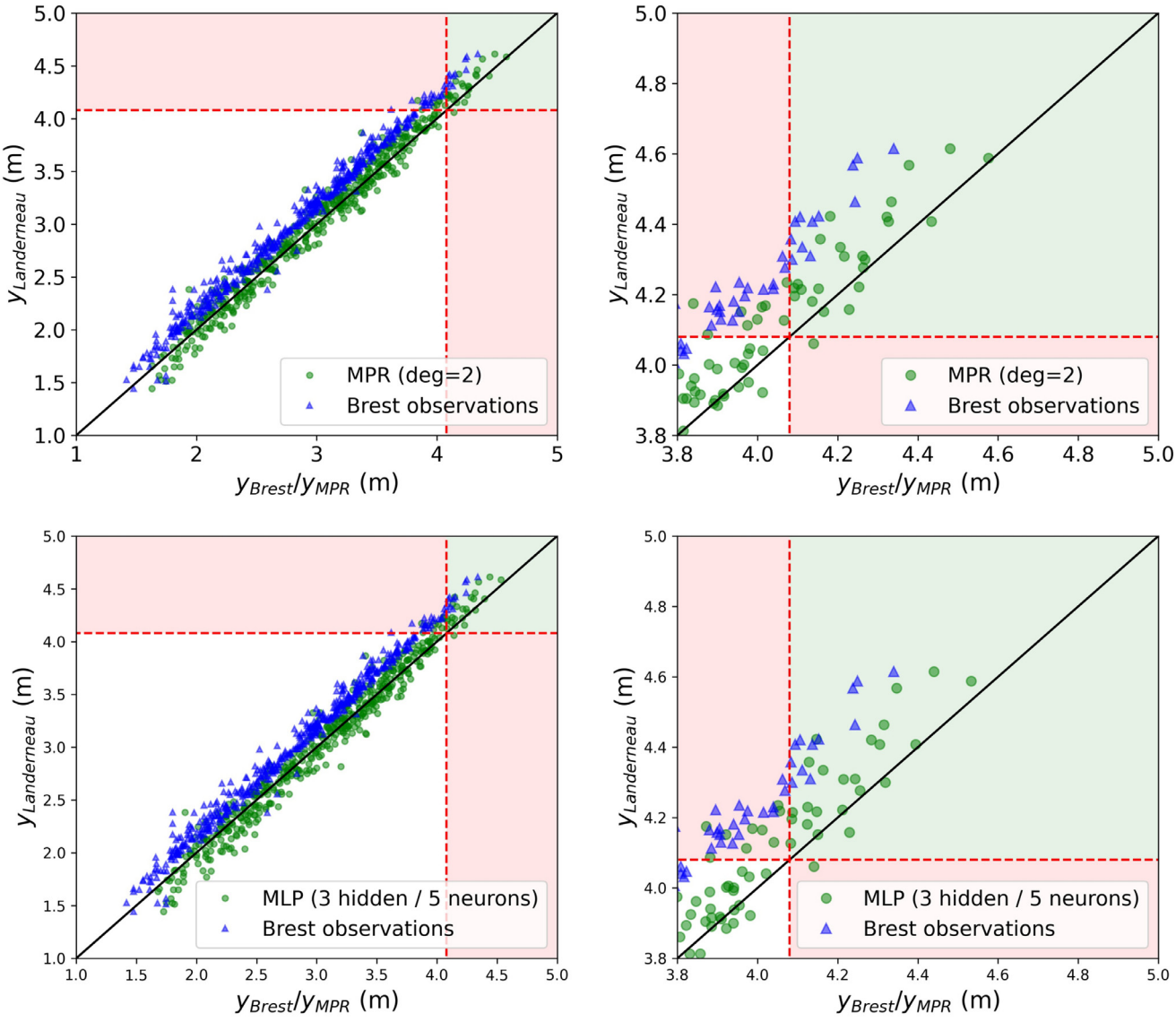

Figure 11 Correlation between maxima observed and predicted — from (top) MPR with deg=2 and (bottom) MLP with 3 hidden layers and 5 neurons per layer — during high tides in the city of Landerneau (green circles). Correlation between maxima observed in Landerneau and in Brest harbour are shown with blue triangles. These different values were shown for the new tested dataset corresponding to the final 30% of observations over the period 02-03-2017/25-06-2020. Two areas were coloured with respect to the approach of inundation events (here shown for a critical value of 4.08 m): (i) Green areas where predictions inform about inundations and (ii) red areas where inundations are not captured by machine learning models.

Table 6 Scoring for the evaluation of peak sea levels during high tides in the city of Landerneau for the MPR with a polynomial regression function of degree two and the ratio 70:30% of the total dataset for training and testing.

Input variables	MAE	RMSE	R^2	# of inundation events captured
C_{tide}, P_{atmos}, $Wind_{proj}$, $River_{flow}$	0.094 m	0.118 m	0.972	69.7%
C_{tide}, P_{atmos}, $Wind_{proj}$	0.095 m	0.119 m	0.972	69.7%
C_{tide}, $River_{flow}$	0.148 m	0.183 m	0.933	65.0%
C_{tide}, $Wind_{proj}$	0.145 m	0.181 m	0.935	63.1%
C_{tide}, P_{atmos}	0.099 m	0.129 m	0.967	75.7%
C_{tide}	0.157 m	0.200 m	0.920	65.0%

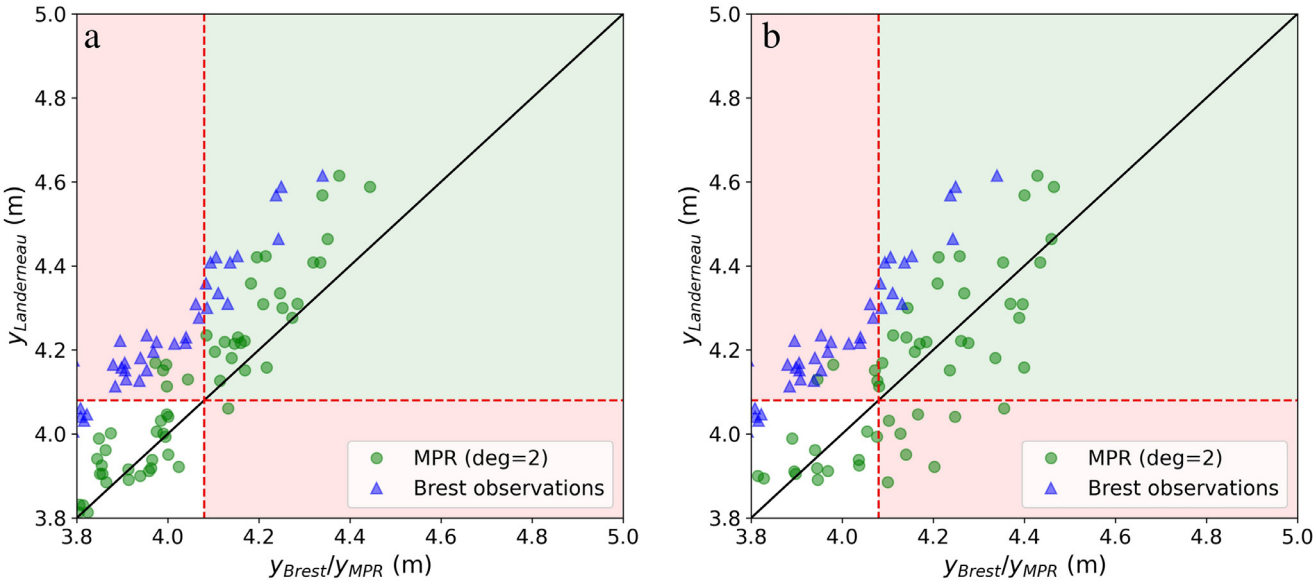

Figure 12 Correlation between observed and predicted maxima during high tides in the city of Landerneau from MPR with deg=2 for (a) C_{tide} and P_{atmos} and (b) C_{tide} as input variables. Correlation between maxima observed in Landerneau and in Brest harbour are shown with blue triangles. These different values were shown for the new tested dataset corresponding to the final 30% of observations over the period 02-03-2017/25-06-2020.

ries of hydrodynamic and hydrological forcings and associated physical processes which interact over a wide range of spatio-temporal time scales. Trained algorithms may therefore show increased uncertainties if these processes are not initially captured by past observations. Moreover, we may expect future change to these physical processes. This clearly restricts the exploitation of machine learning algorithms for forecasting future inundation events, especially over a long time horizon. These algorithms may therefore gain in confidence by exploiting an extensive period of observations (able to capture a wide range of forcings and physical processes) with forecast applications restricted to a limited time horizon.

4. Conclusion

The capability of state-of-the-art machine learning algorithms was assessed for the predictions of sea levels maxima during high tides in the upper part of a tidal estuary of western Brittany (France). The application was dedicated to the Elorn river in the bay of Brest and the city of Landerneau. Such investigation is of high interest for city services which must face frequent river overflows and inundations during high tides. The attention was dedicated to (i) multiple regression methods based on linear and polynomial regression functions, and (ii) an artificial neural network, the multilayer perceptron. A series of four input variables was considered for these algorithms, thus integrating the French tidal coefficient, the atmospheric pressure, the wind velocity and the upstream river discharge. A calibration study was conducted to investigate the performance of the different models with respect to a series of hyperparameters including among others, for ANN, the number of hidden layers and neurons per layer. Particular attention was finally dedicated to the evaluation of river overflows and inundations, identified for maximum sea levels above a given threshold value. The main outcomes of the present investigation are as follows:

1. Results obtained exhibited the improved approach of maxima sea levels variations at both diurnal and spring-neap time scales in the upper part of the estuary, thus integrating the deformation of tide along its propagation, and the global and local meteorological effects. Benefits of such an approach were particularly noticeable when compared to the exploitation of downstream available data (such as observations or offshore predictions).
2. Whereas reduced differences were obtained between the different machine learning models and parametrisations considered, slightly better estimates were predicted for the multiple polynomial regression (with a regression function of degree two) and the multilayer perceptron with three hidden layers and five neurons per layer.
3. Models were furthermore found to slightly underestimate highest sea levels. This tendency impacted the characterisation of inundation events, especially for maxima sea levels close to the threshold value retained for river outflows in the city of Landerneau.
4. A sensitivity study to input variables exhibited the importance of the atmospheric pressure on models performances. Thus, the inclusion of tidal coefficient and atmospheric pressure showed reduced differences in comparison to the integration of the four input variables (including the wind velocity and upstream river discharge). It even resulted in an improved approach of inundation events in the city of Landerneau. Such a result exhibited furthermore the reduced effects of wind and river flows on sea level variations and inundation at the location considered in the city.
5. The practicability of these different algorithms was finally exhibited. Thus, it was possible to approach, with

reduced uncertainties, sea levels variations in the upper part of the estuary by relying on input variables extracted from large-scale database repository. And this result promotes the application of these advanced methods to forecast inundation in such environments by exploiting short-term weather predictions.

The evolution of sea levels in the upper part of a tidal estuary may therefore be approached with basic multiple regression methods and artificial neural networks which exploit the complex relationships and/or connections between a series of variables without any further hypothesis. Thus, these algorithms were able to integrate, from long-term observations, a series of non-linear phenomenon including the deformation of the tide along its propagation in the estuary or the local interaction with urban docks, and this with a reduced computational effort. These results were obtained by exploiting a three-year long time series of observations, and we may expect further results with a longer time period derived from this instrumentation system. This investigation may also be complemented by exploiting predictions of a refined hydrodynamic model of tidal and coastal surge propagation in the Elorn estuary and the city of Landerneau. Indeed, machine learning algorithms make it difficult to encompass the physical mechanisms involved in the evolution of upstream sea levels. Thus, beyond a simple analysis of advantages/drawbacks for sea levels predictions, numerical modelling will provide further insights about the global and local processes controlling the inundation in the city of Landerneau of great interest for remedy solutions. Such investigation may also be continued by implementing a hybrid approach forcing the numerical model with predictions from machine learning algorithms.

CRediT authorship contribution statement

Nicolas Guillou: Conceptualization, Methodology, Software, Validation, Formal analysis, Investigation, Writing — original draft, Writing — review & editing, Visualization, Supervision, Project administration. **Georges Chapalain:** Writing — review & editing, Project administration.

Acknowledgements

The present paper is a contribution to the research program INTERIMER (“INTEractions entre RIvière(s) et MER”) of the Laboratory of Coastal Engineering and Environment (Cerema, http://www.cerema.fr). The authors thank Olivier Boucher and Antoine Douchin from the research team for their technical support in setting up the instrumentation system in the city of Landerneau.

References

Ali, M., Prasad, R., Xiang, Y., Deo, R.C., 2020. Near real-time significant wave height forecasting with hybridized multiple linear regression algorithms. Renew. Sust. Ener. Rev. 132, 110003. https://doi.org/10.1016/j.rser.2020.110003

Asma, S., Sezer, A., Ozdemir, O., 2012. MLR and ANN models of significant wave height on the west coast of India. Computers & Geosciences 49, 231—237. https://doi.org/10.1016/j.cageo.2012.05.032

Azencott, C.A., 2019. Introduction au Machine Learning. Dunod Dunod, Cambridge, UK, 240 pp.

Banque Hydro, 2021. Banque Hydro. http://hydro.eaufrance.fr/indexd.php (accessed on 03/2021).

Beudin, A., Chapalain, G., Guillou, N., 2014. Modelling dynamics and exchanges of fine sediments in the bay of Brest. La Houille Blanche 6, 47—53. https://doi.org/10.1051/lhb/2014062

Beuzen, T., Splinter, K., 2020. chapter Machine learning and coastal processes. Elsevier, 689—710. https://doi.org/10.1016/B978-0-08-102927-5.00028-X

Cerema-LGCE, 2021. https://www.cerema.fr/fr/cerema/directions/cerema-eau-mer-fleuves/lgce (accessed on 03/2021).

Chao, W.T., Young, C.C., Hsu, T.W., Liu, W.C., Liu, C.Y., 2020. Long-lead-time prediction of storm surge using artificial neural networks and effective typhoon parameters: Revisit and deeper insight. Water 12. https://doi.org/10.3390/w12092394

Deo, M., Jha, A., Chaphekar, A., Ravikant, K., 2001. Neural networks for wave forecasting. Ocean Eng. 28, 889—898. https://doi.org/10.1016/S0029-8018(00)00027-5

Fan, S., Xiao, N., Dong, S., 2020. A novel model to predict significant wave height based on long short-term memory network. Ocean Eng. 205, 107298. https://doi.org/10.1016/j.oceaneng.2020.107298

Feng, X., Ma, G., Su, S.F., Huang, C., Boswell, M.K., Xue, P., 2020. A multi-layer perceptron approach for accelerated wave forecasting in Lake Michigan. Ocean Eng. 211, 107526. https://doi.org/10.1016/j.oceaneng.2020.107526

French, J., Mawdsley, R., Fujiyama, T., Achuthan, K., 2017. Combining machine learning with computational hydrodynamics for prediction of tidal surge inundation at estuarine ports. Procedia IUTAM 25, 28—35. https://doi.org/10.1016/j.piutam.2017.09.005

Hashemi, M.R., Spaulding, M.L., Shaw, A., Farhadi, H., Lewis, M., 2016. An efficient artificial intelligence model for prediction of tropical storm surge. Nat. Hazards 82, 471—491. https://doi.org/10.1007/s11069-016-2193-4

Humphrey, G.B., Gibbs, M.S., Dandy, G.C., Maier, H.R., 2016. A hybrid approach to monthly streamflow forecasting: Integrating hydrological model outputs into a bayesian artificial neural network. J. Hydrol. 540, 623—640. https://doi.org/10.1016/j.jhydrol.2016.06.026

Keras, 2021. Keras, Simple. Flexible. Powerful. keras.io (accessed on 03/2021).

Kingma, D.P., Ba, J.L., 2015. Adam: A Method for Stochastic Optimization. International Conference on Learning Representations.

Kumar Paramasivan, S., 2019. Improved Prediction of Wind Speed using Machine Learning. EAI Endorsed Transactions on Energy Web 7. https://doi.org/10.4108/eai.13-7-2018.157033

Lee, T.L., Jeng, D.S., 2002. Application of artificial neural networks in tide-forecasting. Ocean Eng. 29, 1003—1022. https://doi.org/10.1016/S0029-8018(01)00068-3

Liu, J., Shi, G., Zhu, K., 2019. High-precision combined tidal forecasting model. Algorithms 12. https://doi.org/10.3390/a12030065

Manero, J., Béjar, J., Cortés, U., 2019. Deep Learning is blowing in the wind. Deep models applied to wind prediction at turbine level. IOP Conf. Series: J. Phys. 1222. https://doi.org/10.1088/1742-6596/1222/1/012037

Messikh, N., Bousba, S., Bougdah, N., 2017. The use of a multilayer perceptron (MLP) for modelling the phenol removal by emulsion liquid membrane. J. Environ. Chem. Eng. 5, 3483—3489. https://doi.org/10.1016/j.jece.2017.06.053

Nair, V., Hinton, G.E., 2010. Rectified linear units improve restricted boltzmann machines. In: Proceedings of the 27th

International Conference on Machine Learning (ICML-10), 807—8014.

NOAA, 2021. Climate Forecast System (CFS). https://www.ncdc.noaa.gov/data-access/model-data/model-datasets (accessed on 03/2021).

Noori, N., Kalin, L., 2016. Coupling SWAT and ANN models for enhanced daily streamflow prediction. J. Hydrol. 533, 141—151. https://doi.org/10.1016/j.jhydrol.2015.11.050

Peng, M., Xie, L., Pietrafesa, L.J., 2004. A numerical study of storm surge and inundation in the Croatan-Albemarle-Pamlico Estuary System. Estuar. Coast. Shelf S. 59, 121—137. https://doi.org/10.1016/j.ecss.2003.07.010

Pinheiro, J.P., Lopes, C.L., Ribeiro, A.S., Sousa, M.C., Dias, J.M., 2020. Tide-surge interaction in Ria de Aveiro lagoon and its influence in local inundation patterns. Cont. Shelf Res. 200, 104132. https://doi.org/10.1016/j.csr.2020.104132

Renosh, P.R., Jourdin, F., Charantonis, A.A., Yala, K., Rivier, A., Badran, F., Thiria, S., Guillou, N., Leckler, F., Gohin, F., Garlan, T., 2017. Construction of multi-year time-series profiles of suspended particulate inorganic matter concentrations using machine learning approach. Remote Sens. 9. https://doi.org/10.3390/rs9121320

Rezaeianzadeh, M., Tabari, H., Yazdi, A., Isik, S., Kalin, L., 2013. Flood flow forecasting using ANN, ANFIS and regression models. Neural Comput. Appl. 25. https://doi.org/10.1007/s00521-013-1443-6

Saha, S., Moorthi, S., Wu, X., Wang, J., Nadiga, S., Tripp, P., Behringer, D., Hou, Y.T., Chuang, H., Iredell, M., Ek, M., Meng, J., Yang, R., Mendez, M.P., van den Dool, H., Zhang, Q., Wang, W., Chen, M., Becker, E., 2014. The NCEP Climate Forecast System Version 2. J. Climate 27, 2185—2208. https://doi.org/10.1175/JCLI-D-12-00823.1

Sahoo, B., Bhaskaran, P.K., 2019. Prediction of storm surge and coastal inundation using Artificial Neural Network - A case study for 1999 Odisha Super Cyclone. Weather Clim. Extr. 23, 100196. https://doi.org/10.1016/j.wace.2019.100196

Shih, S.S., Kuo, P.H., Lai, J.S., 2019. A nonstructural flood prevention measure for mitigating urban inundation impacts along with river flooding effects. J. Environ. Manage. 251, 109553. https://doi.org/10.1016/j.jenvman.2019.109553

SHOM, 2021. https://www.data.shom.fr (accessed on 03/2021).

Simon, B., 2007. La marée - La marée océanique côtière. Institut Océanographique, 433 pp.

Tréguer, P., Goberville, E., Barrier, N., L'Helguen, S., Morin, P., Bozec, Y., Rimmelin-Maury, P., Czamanski, M., Grossteffan, E., Cariou, T., Répécaud, M., Quéméner, L., 2014. Large and local-scale influences on physical and chemical characteristics of coastal waters of Western Europe during winter. J. Marine Syst. 139, 79—90. https://doi.org/10.1016/j.jmarsys.2014.05.019

Tsakiri, K., Marsellos, A., Kapetanakis, S., 2018. Artificial Neural Network and Multiple Linear Regression for Flood Prediction in Mohawk River, New York. Water 10. https://doi.org/10.3390/w10091158

Wang, S., Mu, L., Liu, D., 2021a. A hybrid approach for El Niño prediction based on Empirical Mode Decomposition and convolutional LSTM Encoder-Decoder. Comput. Geosci. 149, 104695. https://doi.org/10.1016/j.cageo.2021.104695

Wang, Y., Chen, J., Cai, H., Yu, Q., Zhou, Z., 2021b. Predicting water turbidity in a macro-tidal coastal bay using machine learning approaches. Estuar. Coast Shelf S. 107276. https://doi.org/10.1016/j.ecss.2021.107276

Wang, Z.B., Vandenbruwaene, W., Taal, M., Winterwerp, H., 2019. Amplification and deformation of tidal wave in the Upper Scheldt Estuary. Ocean Dynam. 69, 829—839. https://doi.org/10.1007/s10236-019-01281-3

WMO, 2021. World Meteorological Organization. Données d'observation des principales stations météorologiques https://www.data.gouv.fr/fr/datasets/donnees-d-observation-des-principales-stations-meteorologiques/ (accessed on 03/2021).

Wolff, S., O'Donncha, F., Chen, B., 2020. Statistical and machine learning ensemble modelling to forecast sea surface temperature. J. Marine Syst. 208, 103347. https://doi.org/10.1016/j.jmarsys.2020.103347

Wöppelmann, G., Pouvreau, N., Coulomb, A., Simon, B., Woodworth, P.L., 2008. Tide gauge datum continuity at Brest wince 1711: France's longest sea-level record. Geophys. Res. Lett. 35. https://doi.org/10.1007/s10236-005-0044-z